energies

MDPI

Article

Energy Performance Evaluation of Shallow Ground Source Heat Pumps for Residential Buildings

Archan Shah [1], Moncef Krarti [1,*] and Joe Huang [2]

[1] Department of Civil, Environmental and Architectural Engineering, University of Colorado Boulder, Boulder, CO 80309, USA; archan.shah@colorado.edu
[2] White Box Technologies, Moraga, CA 94556, USA; yjhuang@whiteboxtechnologies.com
* Correspondence: krarti@colorado.edu

Abstract: This paper evaluates the energy performance of shallow ground source heat pumps using the state-of-art whole building energy simulation tool. In particular, the paper presents a systematic and easy to implement approach to model the energy performance of shallow and helical ground heat exchangers and assess their energy efficiency benefits to heat and cool buildings. The modeling approach is based on the implementation of G-functions, generated using a validated numerical model, in a state-of-art whole building energy simulation tool. Both the numerical model and the simulation tool are applied to assess the energy performance of various shallow geothermal systems designed to meet heating and cooling needs for detached single-family homes in California. Specifically, a series of sensitivity analyses is conducted to determine the energy performance of the shallow geothermal systems in 16 locations representing all California climate zones. It is found that the suitability and the efficiency of the shallow geothermal systems vary widely and depend on several factors including their design specifications as well as the climate conditions. Compared with conventional air-to-air heat pumps, the shallow ground source heat pumps can be more energy efficient in most climate zones in California except those locations with extreme weather conditions resulting in either heating or cooling only operation. Moreover, configurations of shallow ground source heat pumps with 16 boreholes with 6.7 m (22 ft) depth are found to be cost-effective in several California climate zones.

Keywords: energy efficiency; residential building; shallow ground source heat pump; vertical boreholes

Citation: Shah, A.; Krarti, M.; Huang, J. Energy Performance Evaluation of Shallow Ground Source Heat Pumps for Residential Buildings. *Energies* **2022**, *15*, 1025. https://doi.org/10.3390/en15031025

Academic Editor: Dorota Chwieduk

Received: 20 November 2021
Accepted: 19 January 2022
Published: 29 January 2022

1. Introduction

Ground medium with its deep temperature that remains constant throughout the year has a large capacity to store heating and cooling energy. Thus, the ground has been utilized to passively heat and cool dwellings by several civilizations over thousands of years [1]. More recently, the ground is used as a heat source and sink for ground source heat pumps (GSHPs) to heat and cool buildings [2]. Indeed, GSHPs transfer heat from the ground medium to the building during heating modes but operate in reverse by extracting heat from the building indoors to release it into the ground during cooling modes. Effectively, GSHPs utilize renewable energy stored within the ground medium to meet the heating and cooling needs of buildings. Moreover, GSHPs have several advantages when compared with conventional mechanical heating, ventilating, and air conditioning (HVAC) systems [2,3]. Some of these advantages include lower operating and maintenance costs, quieter operation, and low environmental impact. It is estimated that GSHPs use one unit of electricity to transfer five times the equivalent heat units from the ground [3]. For space cooling applications, the performance of GSHPs is characterized by their electric efficiency ratio (EER) that can exceed 24, or twice that of conventional air-conditioning systems. As a result, the energy demands and thus the operating costs and greenhouse

emissions of GSHPs are generally lower than those incurred by other conventional HVAC systems [4–6]. In particular, GSHPs can reduce by 50% HVAC energy consumption when compared with conventional systems [4].

Many studies and analyses have been reported worldwide to optimize the design configurations and evaluate the benefits associated with GSHPs [7]. For instance, Ma et al. [8] evaluated the energy and environmental benefits of the GSHP in the Wuhan region for summer conditions. Their study indicated that GSHPs reduce by 43.9% annual energy for heating and cooling end-uses when compared with conventional coal-fired boilers and water-cooled chillers. Similarly, Michopoulos et al. [9] have evaluated the energy, environmental and economic benefits of GSHP installations for residential homes in Cyprus. The analysis was carried out using a whole-building energy simulation tool to compare the performance of the conventional systems with the vertical GSHPs as well as of water-to-water heat pumps. More recently, GSHPs with very deep boreholes using 1500 m to 3000 m wells have been proposed since they require significantly less land and more effectively utilize deep soil stored energy than the systems with typical borehole depths of 100 m to 150 m [10,11]. The energy performance of these deep GSHPs have been evaluated using numerical models that were experimentally validated [12,13]. These models have been utilized to determine the design and operating parameters that most affect the energy efficiency of deep GSHPs [14]. The results of reported studies for systems with both typical and deep boreholes show that the implementation of GSHPs results in a decrease in energy consumption and an increase in economic benefits for favorable locations. While most of the studies have confirmed the high energy efficiency potential of GSHPs compared with conventional heating and cooling systems, they noted that the high installation costs represent the main hindrance to their wide penetration for several regions of the world including the U.S. [15,16]. Indeed, the drilling cost for the deep vertical boreholes can be a significant factor that affects the cost-effectiveness of GSHPs to be viable options for heating and cooling buildings [17–19]. In the U.S., the drilling cost for a single GSHP borehole is estimated to be USD 49/m (USD 15/ft) of depth [6]. Therefore, the drilling costs for merely two 60 m (200 ft) boreholes for a typical U.S. dwelling requiring 2 tons of cooling can cost up to USD 6000.

Alternatives to GSHPs have been proposed to reduce the drilling costs of deep boreholes for both residential and commercial applications. In particular, thermal piles or thermos-active foundations (TAFs) have been considered mainly for commercial buildings with ground heat exchanger loops that are integrated with the building foundations, eliminating the need to dig for separate GSHP boreholes [20]. Most TAFs consist of heat exchanger loops attached to reinforcement cages of drilled or augured foundations [21,22]. Small diameter TAF tubes are typically utilized to maximize the number of heat exchanger loops per foundation [23,24]. Several studies have evaluated the energy efficiency potential and the techno-economic performance of these systems [25–29]. TAFs have been deployed in several high-rise buildings especially in Europe and Asia but have been rarely installed in the U.S. due to concerns about the structural integrity of the foundations as well as limited data about their energy performance and cost benefits [30].

For residential buildings, shallow GSHPs or S-GSHPs have been considered as a possible alternative to deep borehole GSHPs. S-GSHPs have shallow boreholes with the depth ranging between 3 m to 9 m (i.e., 10 ft to 30 ft) to reduce the drilling costs and avoid excavation through bedrocks, water tables, and other geological features [31]. Only limited analyses have been reported in the literature to determine the best design configurations as well as the cost benefits of S-GSHPs. Most of these analyses are based on numerical modeling of S-GSHP systems using helical heat exchangers to evaluate their energy performance [31–40]. For instance, a CFD-based analysis has demonstrated that the helical shape is the optimal configuration for the ground heat exchanger to maximize the heat extraction rate and minimize borehole depth [31]. Another CFD-based model has been developed and validated using laboratory data for a simplified ground heat exchanger set-up [32]. A finite-element numerical model for a helical heat exchanger is developed

and validated using field data obtained for one borehole and nine spiral heat exchanger loops [33]. Recently, a simplified one-dimensional model has been developed and validated for a shallow helical ground heat exchanger system that is combined with phase change materials to form an underground thermal battery [34]. Moreover, a numerical analysis based on conduction-resistance modeling, referred to as the CaRM model, has been developed to compare the energy performance of helical ground heat exchanger loops with those using double and triple U-tubes and concluded that helical loops have the highest energy performance [38]. The numerical model has been adjusted and compared with CFD analysis results as well as measured data obtained from the standalone ground heat exchanger borehole [39]. The reported analyses suggest that helical-shaped ground heat exchangers can be used as alternatives to conventional U-tube ground heat exchangers to reduce the required borehole depth and consequently lower the installation costs of GSHPs [40]. In a recently reported study, the CaRM model is utilized to assess the cost-effectiveness of S-GSHPs for a housing unit located in two locations in California [41]. The analysis utilizes heating and cooling loads estimated without any HVAC system to estimate the energy demand for the S-GSHP and thus ignores the thermal interactions between thermal loads and heat pump operation. The analysis results show that the S-GSHPs can save about 28% of electricity demand compared with air-to-air heat pumps for both considered locations. However, the analysis indicates that the cost of S-GSHPs has to be reduced by at least 22% to be cost-effective compared with rooftop PV systems [41,42].

While there are several numerical models developed for S-GSHPs, no integrated analysis is carried out to assess the performance of S-GSHPs as part of a whole-building simulation tool. Moreover, no detailed analyses based on whole-building performance have been reported in the literature to determine the optimal design configurations to maximize the energy efficiency and cost benefits of S-GSHPs, especially for U.S. residential buildings. In fact, the state of California has a low rate of adoption of GSHPs despite having the most aggressive U.S. energy standards [6,32]. The study described in this paper aims to demonstrate the application of a new modeling approach that can be readily applied to optimize the design configuration and evaluate the cost-effectiveness of S-GSHPs when deployed to any building and any climate. The modeling approach is based on the integration of the G-functions using the results of numerical modeling of helical ground heat exchangers into a whole-building simulation engine.

Specifically, this paper presents an integrated modeling approach to evaluate the energy performance and the economic feasibility of S-GSHPs to heat and cool residential buildings in 16 climate zones of California. First, the modeling analysis approach is described including the building simulation analysis tool and prototypical detached single-family home characteristics as well as the G-function concept used to model the performance of S-GHSPs. Then, the energy performance of the S-GSHPs is compared with that of the air source heat pumps considered as the baseline systems to heat and cool residential buildings in California. A series of sensitivity analyses is conducted to determine the impact of various design and operating conditions on the performance of S-GSHPs including soil and grout thermal properties as well as borehole depths. Finally, an economic assessment is carried out based on the life-cycle cost analysis method to determine the specific climate zones in California where S-GSHPs can be cost-effective options as heating and cooling systems for residential buildings.

2. Analysis Approach

This section outlines the modeling methods used to assess the energy performance of S-GSHPs for residential buildings in various climate zones of California. Figure 1 illustrates the analysis approach steps considered in this study including data collection for modeling the prototypical residential building as well as associated baseline HVAC and S-GSHP systems, followed by calculations of the G-functions for various S-GSHP options considered in this study. Then, a detailed energy analysis of the residential building considered in this study is conducted using the baseline HVAC and S-GHSP systems with the final step

consisting of evaluating the cost-effectiveness evaluation of deploying S-GHSP instead of the baseline HVAC system.

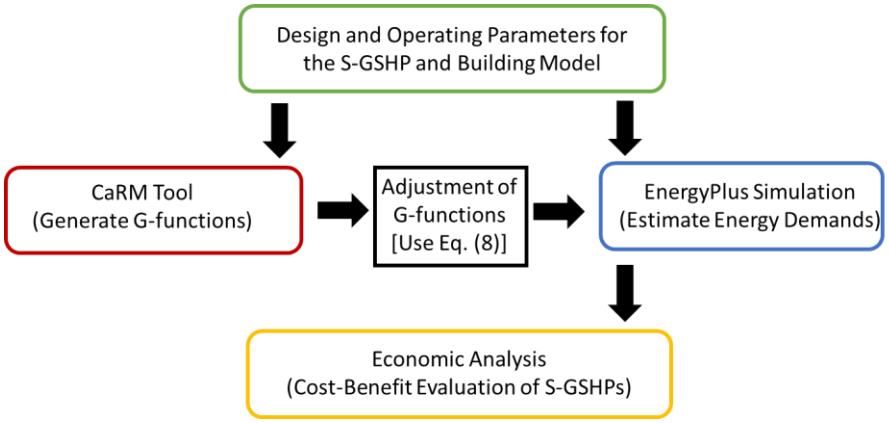

Figure 1. Analysis approach considered to assess the cost-effectiveness of S-GSHP systems.

In this section, the specifications of the residential building used in the analysis are first described. Then, the characteristics of the climate zones considered in the analysis are summarized. Finally, the S-GSHPs thermal modeling using G-functions technique is detailed. The economic analysis and its results are presented in Section 4.

2.1. Building Energy Model

The analysis considers the impact of using shallow ground source heat pumps (S-GSHPs) on heating and cooling energy end-uses for a prototypical detached single-family home located in various locations representative of California climate zones. The home has two stories with a total conditioned area of 233 m^2 (2400 ft^2) with a window-to-wall ratio of 15% [43]. Figure 2 shows a three-dimensional rendering of the two-story home model and Table 1 summarizes the main features of the home model considered in EnergyPlus, a state-of-the-art whole-building energy simulation tool used to perform the analysis [44]. The baseline heating and cooling system for the home consists of a direct expansion unitary air-to-air heat pump. All the energy end-uses including those related to lighting, appliances, and HVAC systems are estimated by the simulation tool on any desired time step basis including annual, monthly, hourly, and even sub-hourly [44].

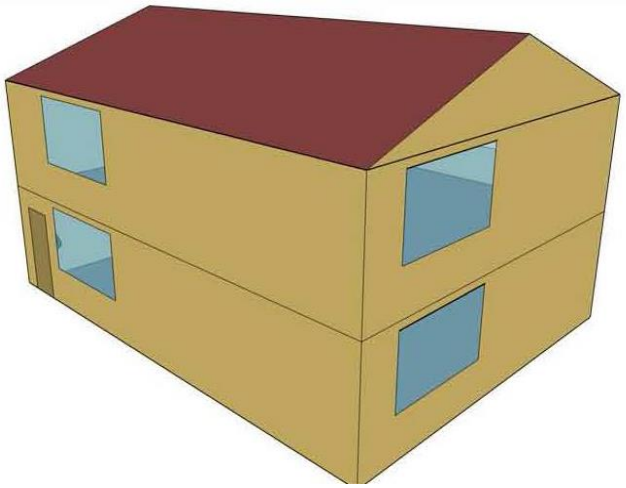

Figure 2. Rendering of the detached home model used in this study.

Table 1. Basic features of the detached home model used for the simulation analysis.

Building Characteristic	Value
General Home Dimensions	
Conditioned floor area	2399 ft^2 (222.9 m^2)
Roof area	1270 ft^2 (117.5 m^2)
Number of stories	2
Window-to-wall ratio	0.15
Wall Area by Orientation	
North	569.2 ft^2 (52.8 m^2)
East	421.8 ft^2 (39.1 m^2)
South	569.2 ft^2 (52.8 m^2)
West	421.8 ft^2 (39.1 m^2)
Foundation Type	Slab-on-grade
Effective Air Leakage Area	
Living space	37.7 ft^2 (3.5 m^2)
Attic	16.6 ft^2 (1.5 m^2)
Lighting and Appliances	
Lighting power density	0.19 W/ft^2 (2.0 W/m^2)
Equipment power density	0.46 ft^2 (5.00 W/m^2)
HVAC System Type	Air-to-Air Heat Pump
HVAC System Efficiency	
COP heating	4.2
COP cooling	3.9

2.2. California Climate Zones

The simulation analysis for the energy performance of the shallow GSHPs is carried out for 16 locations to represent the California climate zones as depicted by the map of Figure 3 [45]. The annual heating and cooling degree days for the selected 16 Californian locations are summarized in Table 2. As noted in Table 2, California includes a wide spectrum of climatic conditions ranging from cold (Arcata and Mount Sasha) to hot (Imperial) weather. However, most zones in California exhibit mild climates with both cooling and heating thermal needs with some dominance of cooling requirements especially for buildings with significant internal loads.

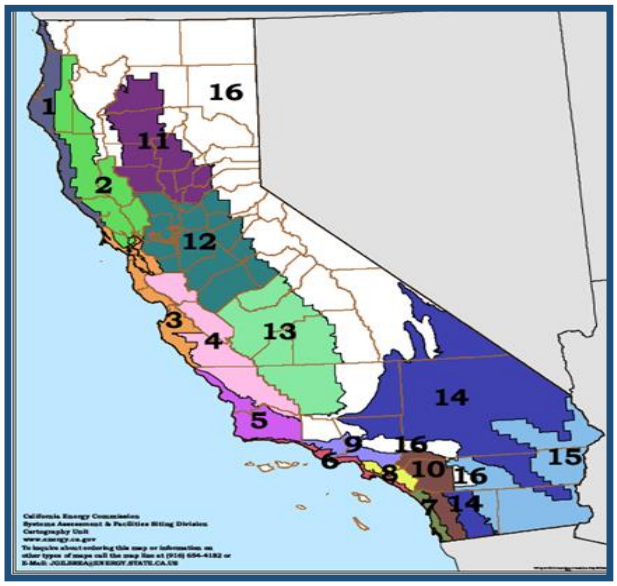

Figure 3. Map for the 16 climate zones for California [45].

Table 2. Summary of annual heating and cooling degree days for 16 locations representative of California climate zones based on 18 °C (65 °F).

Location	HHD (18 °C)	CDD (18 °C)	HHD (65 °F)	CDD (65 °F)
Arcata	2631	0	4999	0
Burbank Glendale–Pasadena	668	861	1269	1636
China Lake	1317	1694	2502	3219
Fresno Yosemite	1104	1431	2098	2719
Fullerton Municipal Airport	524	833	996	1583
Imperial	477	2436	906	4628
Long Beach–Daugherty	647	458	1229	870
March AFB	1180	908	2242	1725
Mount Shasta	3033	339	5763	644
Oakland Metropolitan	1400	75	2660	143
Red Bluff Municipal Airport	1306	1262	2481	2398
Sacramento Executive Airport	1260	702	2394	1334
San–Diego–Lindbergh	516	462	980	878
San Jose International Airport	1296	159	2462	302
Santa Maria Public Airport	1394	69	2649	131
Santa Rosa	1580	227	3002	431

2.3. Helical S-GSHP Modeling

There are two main components of a typical ground source heat pump including the interior equipment and the ground heat exchangers also referred to as ground heat exchange loops. The interior equipment consists of the heat pump and associated distribution systems to provide heating and cooling to the house, while the ground heat exchange loops are designed to extract or reject heat with the ground medium. For most GSHPs, vertical boreholes are used for the ground heat exchange loops rather than horizontal loops due to their higher energy performance. Specifically, vertical GSHPs use U-tube ground heat exchangers to extract and reject heat between the ground the fluid circulating in the loops. Typically, conventional U-tube vertical GSHPs have eight to ten boreholes that have single or double U-tubes carrying working fluid to exchange heat with the ground. Each borehole consists of a U-tube of 20–40 mm diameter and a length of 20–200 m depending on the depth of the borehole.

For this study, a closed-loop helical ground heat exchanger placed in a very shallow vertical borehole as depicted in Figure 4a is considered for the analysis instead of the conventional U-shaped borehole heat exchanger shown in Figure 4b. The helical shallow pipe has an inside diameter of 17.3 mm and an outside diameter of 22.2 mm with a pitch of 0.2286 m. For the conventional U-Tube GSHPs, the diameter of the borehole ranges typically between 0.1 m and 0.2 m. However, for the helical heat exchangers used in this analysis, the diameter of the borehole is considered to be 0.914 m to reduce thermal interactions between loops. The depth of the borehole for the S-GSHP used in this analysis is set to be 22 ft (6.7 m) or 13 ft (3.96 m) depending upon the S-GSHP design configuration [40,41]. Moreover, the depth of the head at the top of the borehole is set to be 1 m below the ground in the analysis performed for this study.

The specific characteristics of the ground heat exchanger along with the site-specific soil thermal properties are used with the CaRM model (conduction resistance model) developed by Zerella et al. [26,30] to determine the G-function coefficient for the S-GSHPs. As noted earlier, the CaRM model has been extended and validated using experimental data to evaluate the energy performance of S-GSHPs [41]. Specifically, the CaRM model uses the thermal network solution technique to model the dynamic process of heat exchange between the borehole heat exchanger and the ground. The CaRM can model the impact

of the thermal properties of the ground medium including subsoil and grout layers on the thermal performance of the helical ground heat exchangers. The output variables that can be obtained from the CaRM model include the inlet and the outlet temperature from the ground heat exchanger and the average temperature along the borehole wall. These output parameters are then utilized to calculate the G-functions required as an input for EnergyPlus simulation analysis [43].

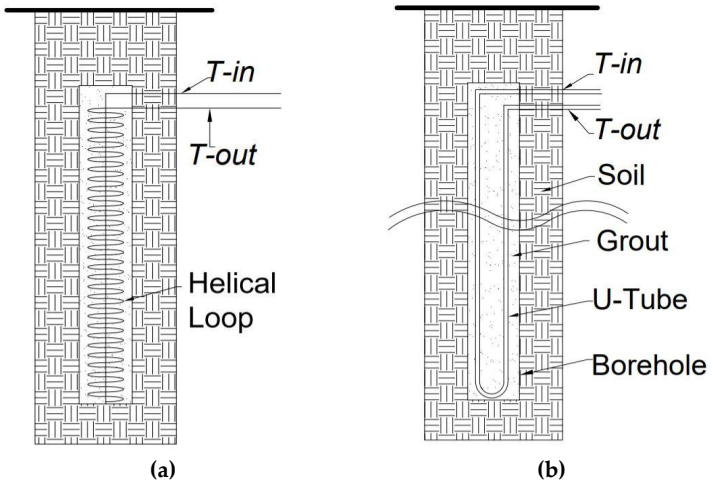

Figure 4. Vertical heat exchangers for (**a**) helical loop (**b**) conventional U-tube.

G-functions consist of long-term and short-term response factors that are often used to model the thermal performance for GSHPs [46–48] and TASFs [49–51] integrated within whole-building simulation tools such as EnergyPlus [43]. Specially, the G-functions can be applied to model the thermal performance of any ground heat exchanger to relate the borehole wall temperature, T_b, to the ground temperature, T_g, and the time variation of the thermal load, $\Delta q_{l,j}$ [46]:

$$T_b = T_g + \sum_{j=1}^{N-1} G_b(r, \theta, t - j\Delta t) \cdot \Delta q_{l,j} \quad (1)$$

For this study, an analytical model helical ground heat exchanger part of the CaRM model is used to compute G-functions that, instead of Equation (1), connect the fluid and ground temperatures [52]. The G-function coefficients, G_f, connecting the fluid temperature T_f, to the ground temperature, T_g, are defined as follows [52]:

$$T_f = T_g + \sum_{j=1}^{N-1} G_f(r, \theta, t - j\Delta t) \cdot \Delta q_{l,j} \quad (2)$$

In Equation (2), (r,θ) are the cylindrical coordinates, t is the time, and j is the counter for the time step Δt. For the simulation tool, EnergyPlus, the G-functions are response factors that connect the borehole wall temperature, T_b, to the ground temperature, T_g, and is denoted as G_b and defined as [43]:

$$T_b = T_g + \sum_{j=1}^{N-1} G_b(r, \theta, t - j\Delta t) \cdot \Delta q_{l,j} \quad (3)$$

where, $\Delta q_{l,j}$ is the thermal load at time step j.

Moreover, the fluid temperature, T_f, is related to the borehole wall temperature, T_b, and the thermal load, q_l, through the effective fluid to borehole wall thermal resistance, $R_{e,b}$ [53]:

$$T_f = T_b + q_l \cdot R_{e,b} \quad (4)$$

The calculation of $R_{e,b}$ involved three main thermal resistances including the fluid convection, the pipe thermal resistance, and the backfill thermal resistance as detailed in [40]. Based on Equation (4), the following equation can be set:

$$T_f = T_b + q_l \cdot R_{e,b} = T_g + \sum_{j=1}^{N-1} G_b(r, \theta, t - j\Delta t) \cdot \Delta q_{l,j} + q_l \cdot R_{e,b} \quad (5)$$

However, using the Hessian function, *He* [*He(t)* = 1 if $t > 0$ and *He(t)* = 0 if $t < 0$], Δq_l, can be expressed as:

$$\Delta q_l(t) = \sum_{j=1}^{N-1} He(t - j\Delta t) \cdot \Delta q_{l,j} \quad (6)$$

Thus,

$$T_f = T_b + \sum_{j=1}^{N-1} [G_b(r, \theta, t - j\Delta t) + He(t - j\Delta t) \cdot R_{e,b}] \, \Delta q_{l,j} \quad (7)$$

Since G_f has been estimated, the proper G-function used by EnergyPlus can be determined by using the formula:

$$G_b(r, \theta, t - j\Delta t) = G_f(r, \theta, t - j\Delta t) - He(t - j\Delta t) \cdot R_{e,b} \quad (8)$$

Based on Equation (8), the G-function coefficients can be calculated for a different number of boreholes for the S-GSHPs. Figure 5 illustrates the G-functions determined for two borehole depths of S-GSHPs and three soil types. The G-function coefficients are then used as the response factors to model S-GSHPs in EnergyPlus [44].

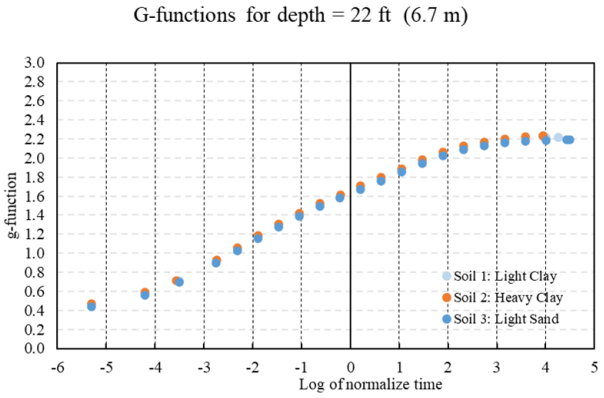

(**a**)

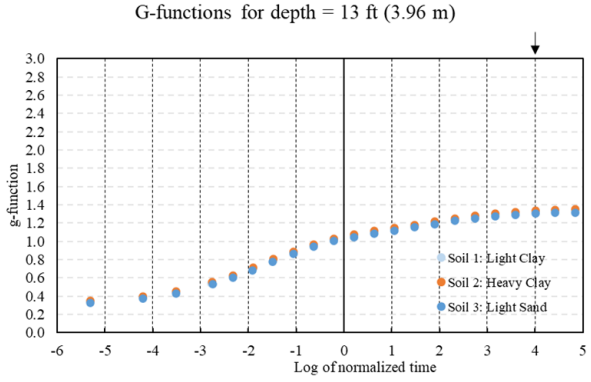

(**b**)

Figure 5. G-function coefficients for various soil types specific to S-GHSP with (**a**) 6.7 m (22 ft) and (**b**) 3.96 m (13 ft) deep boreholes.

3. Discussion of Results

Using EnergyPlus, the house prototypes located in the 16 CA locations are modeled using the baseline heating and cooling system as well as the S-GSHP using the G-function coefficients that have been generated using the CaRM numerical model for various borehole field design configurations and soil thermal properties. In this study, water–propylene glycol (15% by volume), with the thermophysical properties listed in Table 3, was used as a working fluid for the ground heat exchanger [40].

Table 3. Thermophysical properties of the working fluid used for S-GHSP analysis.

Property at 68 °F (20 °C)	Value IP (SI)
Density	63.85 lb/ft^3 (1023 kg/m^3)
Thermal conductivity	0.30 Btu/hr.ft. °F (0.518 W/m·K)
Specific heat	0.928 Btu/lb. °F (3.885 kJ/kg·K)
Viscosity	1.45 cp (1.43 × 10^{-3} Pa·s)
Freezing temperature	22.0 °F (−5.5 °C)
Boiling temperature	215 °F (102 °C)

3.1. Baseline and S-GSHP Energy Performance

In this section, the heating and cooling energy end uses are compared with the baseline air-to-air heat pumps and the S-GSHP systems. For this comparative analysis, the same design settings are assumed for all the locations specific to the S-GSHP including 64 boreholes with 6.7 m (22 ft) depth. This setting is considered to ensure that the refrigerant fluid operates within acceptable temperatures for all the 16 California climate zones. It should be noted that this S-GSHP configuration may not be the optimal design specifications for all locations as demonstrated in the sensitivity analysis outlined in Section 3.2 and the cost-benefit analysis summarized in Section 4. Figure 6 illustrates the heating and cooling thermal loads experienced for one winter week (Figure 6a) and one summer week (Figure 6b) by the baseline and S-GSHP systems for a house located in Sacramento. As expected, the heating thermal load occurs during the winter and is higher during nighttime hours when the outdoor temperature is reduced. Similarly, the cooling thermal loads are higher during late afternoon hours during the summer when the house is occupied, and the outdoor temperatures are highest.

Figure 7 summarizes the comparative analysis of both heating and cooling annual energy end uses between the baseline and S-GSHP systems. As expected, the heating and cooling energy consumptions vary significantly and depend on the climate for each location characterized by its heating and cooling degree days listed in Table 2. In particular, the heating energy use is highest when the house is located at Mount Sasha (with the highest HDD) and lowest at Imperial (with the highest CDD). Conversely, the cooling energy use is highest at Imperial featuring the hottest climate in California. As indicated by the results shown in Figure 7, the S-GSHP consumes less energy for both heating and cooling except for a few locations typically with extreme weather conditions or high deep ground temperatures. When energy end uses for both heating and cooling are added, the S-GSHP consumes less HVAC energy compared with the baseline system in all 16 locations with varying degrees of potential savings as illustrated in Table 4. In particular, the annual energy savings between 12.7 % and 32.9% is achieved when S-GSHP is used instead of the baseline heating and cooling system (i.e., air-to-air heat pump). In most locations, the annual energy savings attributed to S-GSHPs range between 20% and 30%. Better energy and cost benefits could be achieved when the S-GSHP design specifications are optimized as will be discussed in the following sections.

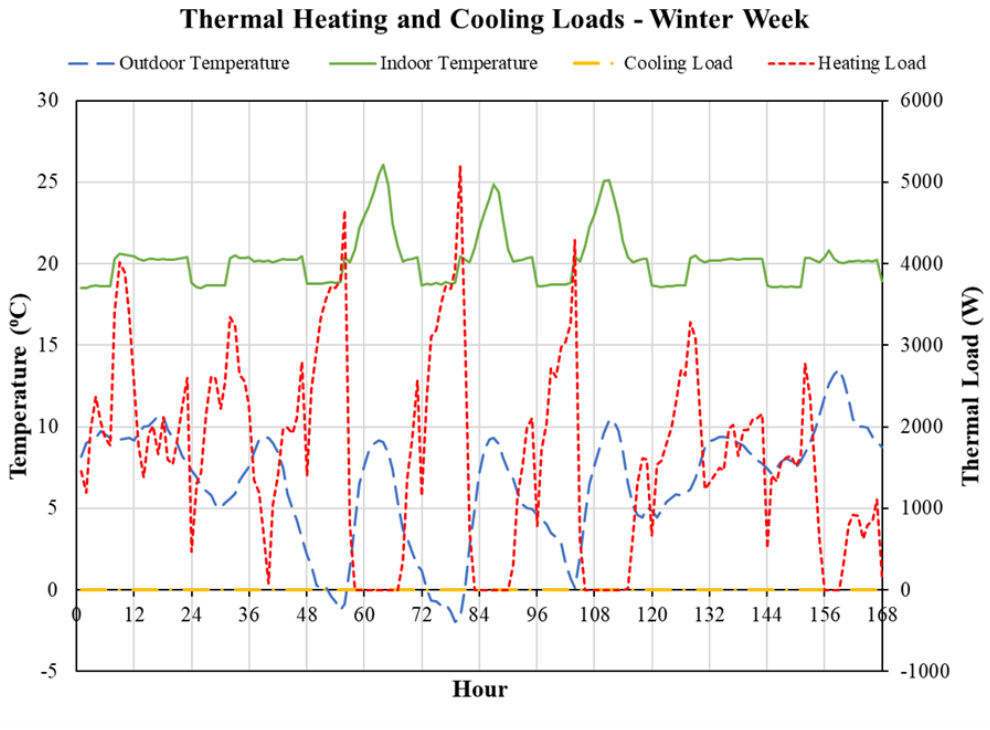

(**a**)

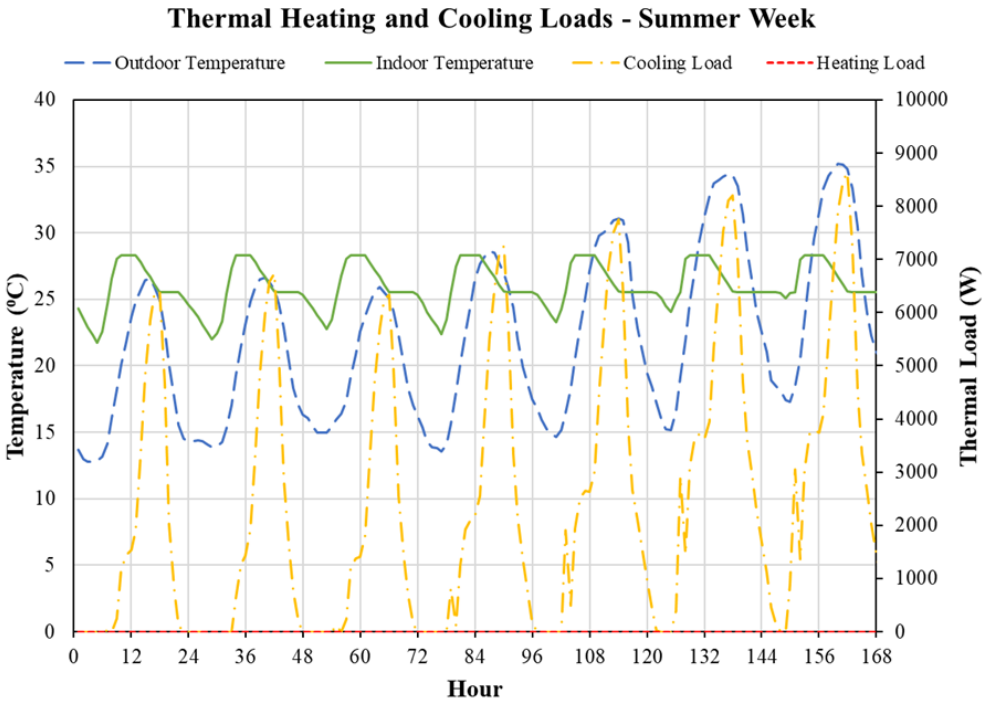

(**b**)

Figure 6. Hourly variations for outdoor and indoor temperatures as well as heating and cooling thermal loads for (**a**) one winter week (i.e., 1–7 January) and (**b**) one summer week (i.e., 15–22 July) for both baseline and S-GSHP systems for a house in Sacramento.

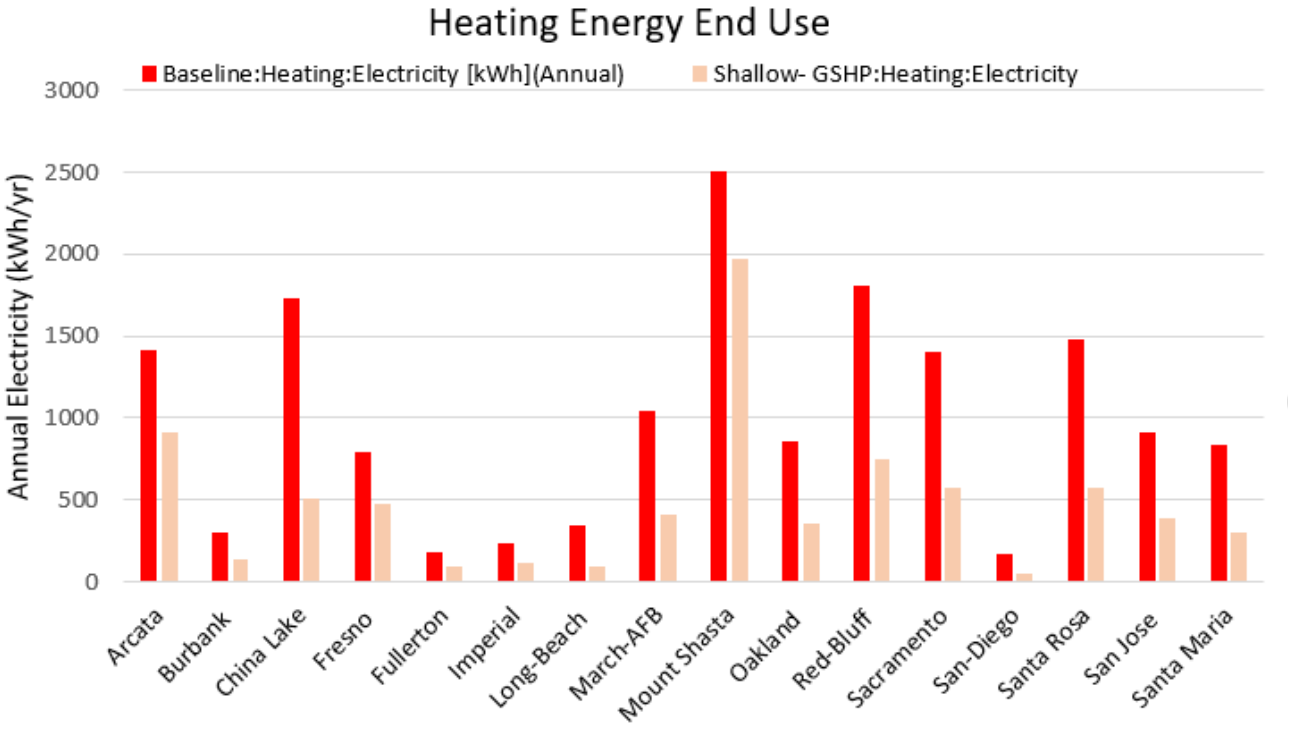

(**a**)

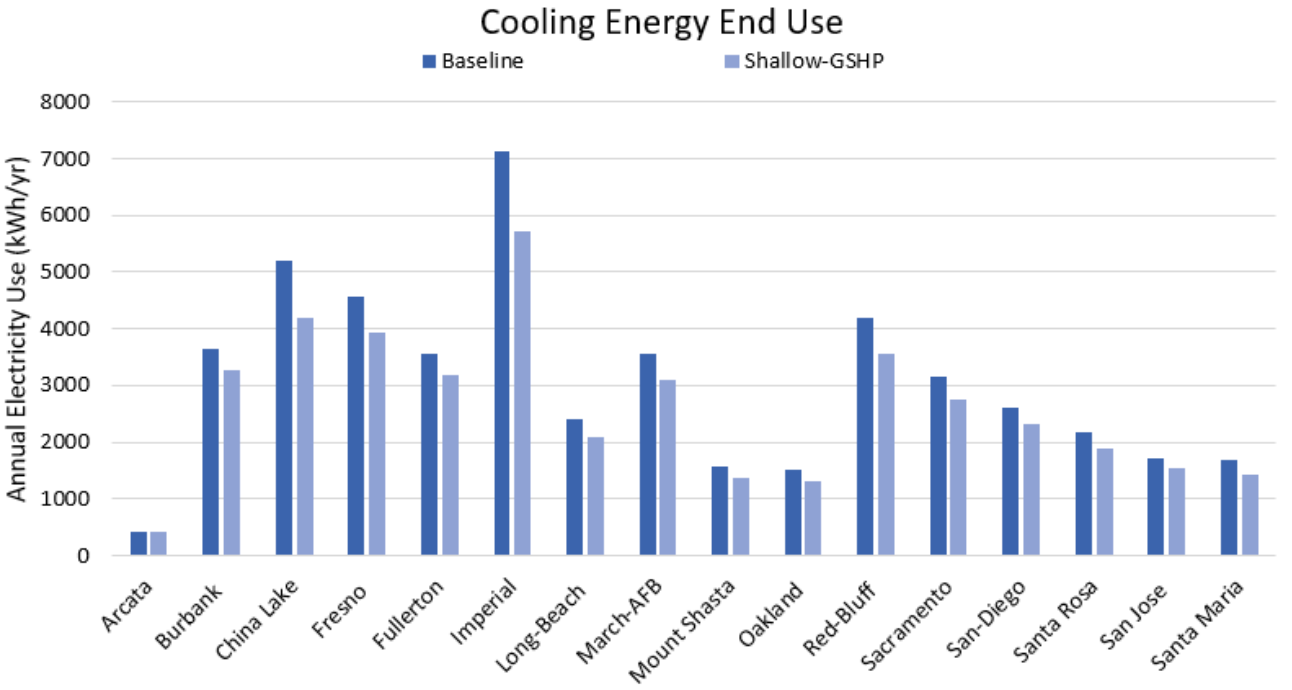

(**b**)

Figure 7. Comparison of annual (**a**) heating and (**b**) cooling electricity end uses associated with baseline and S-GSHP systems for 16 California locations.

Table 4. Annual combined heating and cooling energy consumption for both baseline and shallow GSHP systems for all California locations.

Location	Baseline (kWh)	S-GSHP (kWh)	Percentage Savings (%)
Arcata	1822.21	1315.72	27.8
Burbank	3945.33	3401.37	13.8
China Lake	6920.09	4702.21	32.0
Fresno	5375.82	4417.07	17.8
Fullerton	3741.41	3265.95	12.7
Imperial	7371.03	5816.23	21.1
Long Beach	2756.57	2181.66	20.9
March AFB	4591.56	3500.55	23.8
Mount Shasta	4074.57	3351.13	17.8
Oakland	2378.66	1665.80	30.0
Red Bluff	6005.52	4296.28	28.5
Sacramento	4549.51	3327.88	26.9
San Diego	2767.84	2366.08	14.5
Santa Rosa	3659.72	2455.14	32.9
San Jose	2630.96	1946.31	26.0
Santa Maria	2532.28	1738.20	31.4

3.2. Sensitivity Analysis

Several factors can affect the performance of S-GSHPs to adequately heat and cool buildings including the prototypical house of Figure 1 considered in the study. Indeed, the limited depth of ground-coupled boreholes results in reduced capacity for the S-GSHP system to reject and extract heat to the ground medium and thus effectively meet the building thermal loads. In this section, a series of parametric analyses are presented to gauge the effects of some design parameters and soil conditions on the performance of S-GSHPs to meet heating and cooling requirements for the prototypical house in three CA zones with varying climatic conditions including cold (Arcata), mild (Long Beach), and hot (Imperial).

3.2.1. Effect of Number of Boreholes

The main design parameter for the S-GSHP is the required number of boreholes to meet the thermal loads of the house without experiencing significant overheating and overcooling of the refrigerant fluid circulating in the ground heat exchangers and the heat pump. Figure 8 illustrates the impact of the number of boreholes with 6.7 m (22 ft) depth on the annual heating and cooling end uses. Figure 9 summarizes the results in terms of percent increase relative to the case of 64 boreholes for both heating and cooling energy end uses associated to the house located in three California locations. A few observations can be made based on the results of Figures 8 and 9:

- As expected, when the house is in Arcata (cold climate), the heating energy use is higher than cooling energy consumption. However, when the house is in Long Beach (mild climate) and Imperial (hot climate), the heating energy use is negligible compared with the cooling energy demand indicating that the ground can meet any heating loads for these two locations regardless of the number of boreholes used.
- The higher the number of boreholes, the lower the energy consumption for both heating and cooling end uses. Indeed, the increased number of the boreholes allows the S-GSHP to access higher ground capacity to reject and extract heat. In the cases of lower number of boreholes (i.e., 8 and 16), the temperature refrigerant within the

ground heat exchangers may be outside its recommended operating range. The stars above the bars in Figure 8 indicate cases when the refrigerant temperature is out of the bounds of the recommended operation range.

- When the house is in a cooling-dominated climate such as that of Imperial, the number of boreholes have a significant effect on the energy use of the S-GSHP as illustrated in Figures 8c and 9. Reducing the number of boreholes from 64 to 32 increases the cooling energy end use by 21% while lowering the number of boreholes from 64 to 16 increases the annual energy consumption for cooling by 77% with the refrigerant temperature estimated to be out of the operating range during extended periods.

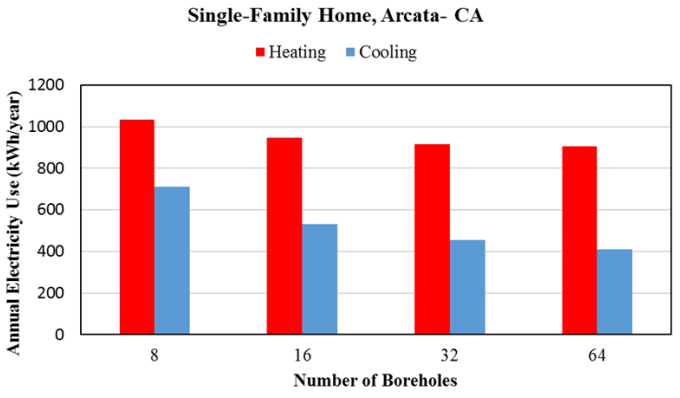

(**a**)

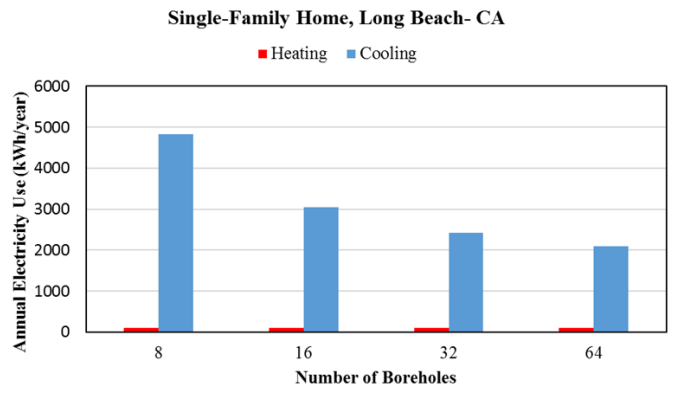

(**b**)

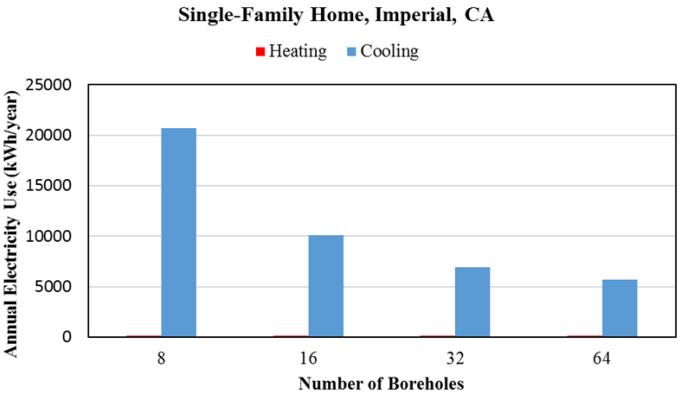

(**c**)

Figure 8. Annual heating and cooling electricity end-uses associated with various numbers of 22 ft (6.7 m) boreholes when the prototypical house is located in (**a**) Arcata, (**b**) Long Beach, and (**c**) Imperial.

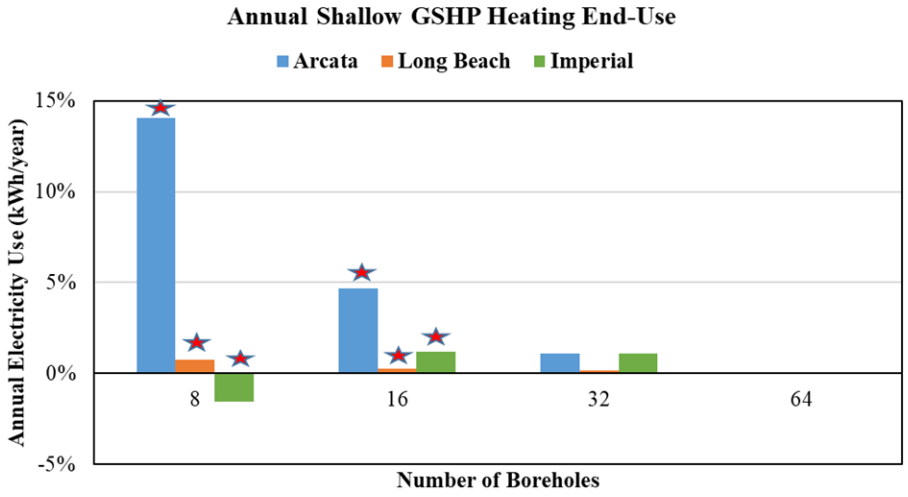

(**a**)

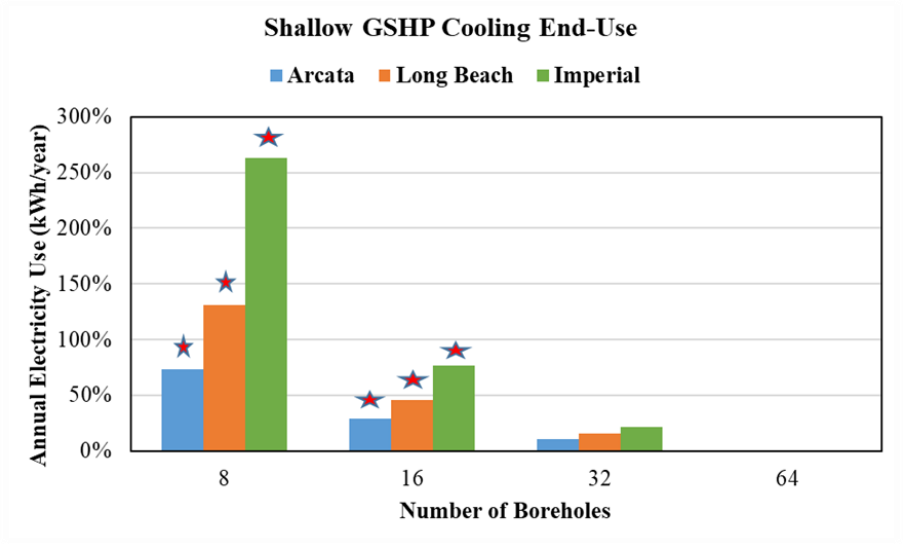

(**b**)

Figure 9. Percent increase relative to the case of 64 boreholes in annual (**a**) heating and (**b**) cooling electricity end uses for various numbers of 6.7 m (22 ft) boreholes when the prototypical house is located in three California locations.

The main takeaway of this analysis is that the number of boreholes should be adequately selected for each location to avoid operation issues as well as to optimally reduce the energy consumption of the S-GHSP.

3.2.2. Effect of the Soil and Grout Thermal Conductivity

As well documented in the literature for ground heat exchangers, soil thermal properties can have a significant effect on the thermal performance and thus the energy use of the S-GSHP. Figure 10 illustrates the impact of four soil thermal conductivity levels on the S-GHSP energy performance for both heating and cooling of the prototypical house located in Long Beach when 32 boreholes are used. For the analysis summarized in Figure 6, the thermal conductivity of the grout around the boreholes is assumed to be the same as that of the ground. As shown in Figure 10, the impact of the soil thermal conductivity, while noticeable, is not significant most likely due to the limited capacity of the ground medium in contact with the boreholes. It should also be noted that the four values of soil thermal conductivity considered in the analysis are specific to properties of common soils in

California [6]. The results indicate that a 50% increase in soil thermal conductivity results in a 10% reduction in S-GSHP cooling energy consumption for a house located in Long Beach.

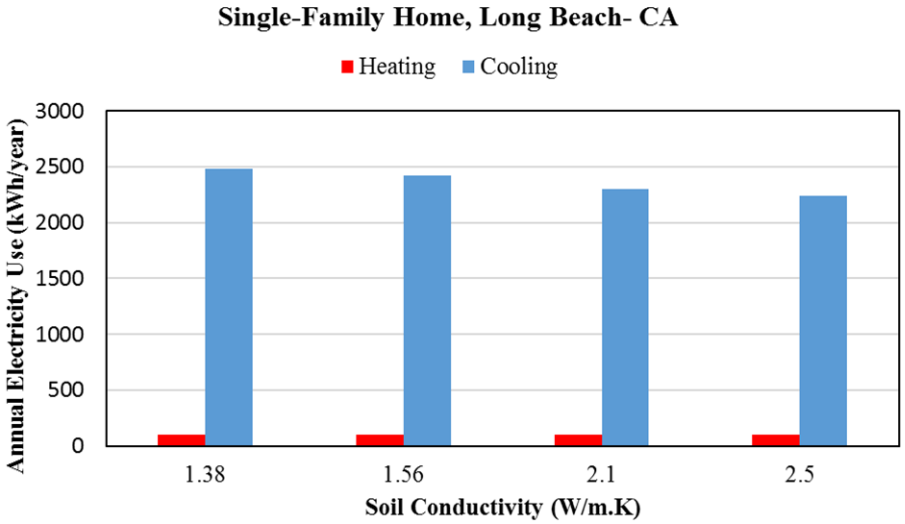

Figure 10. Impact of soil thermal conductivity on annual heating and cooling electricity end uses for 32 boreholes with 6.7 m (22 ft) depth when the prototypical house is located in Long Beach.

In the analysis of Figure 10, the grout thermal conductivity is set to be the same as that of the soil medium. However, it is highly recommended to improve the performance of conventional GSHPs to enhance the thermal properties of the grout around the boreholes to increase heat transfer between the ground medium and the refrigerant. The impact of enhanced grout thermal properties around the boreholes of the S-GSHP is evaluated as summarized in Figure 11 using three ratios of grout-to-soil thermal conductivity values of 1, 1.5, and 2 for the case of 16 boreholes with 6.7 m (22 ft) depth. The results of Figure 11 clearly indicate that the grout thermal properties have a significant impact on the operation and the energy efficiency of the S-GSHP in all three locations considered in the analysis. Indeed, doubling the grout thermal conductivity compared with that of the soil medium decreases both annual cooling and heating energy end uses of the S-GHSP by 75% when the house is located in Long Beach and Imperial. For the case of Arcata, enhanced grout thermal conductivity decreases the cooling consumption by 14% and the heating by 2.5%. Moreover, the refrigerant fluid operates within the recommended temperature range for the cases when the grout thermal conductivity is enhanced, as shown in Figure 11, where the stars indicate instances where the refrigerant temperature becomes out of the acceptable operation range.

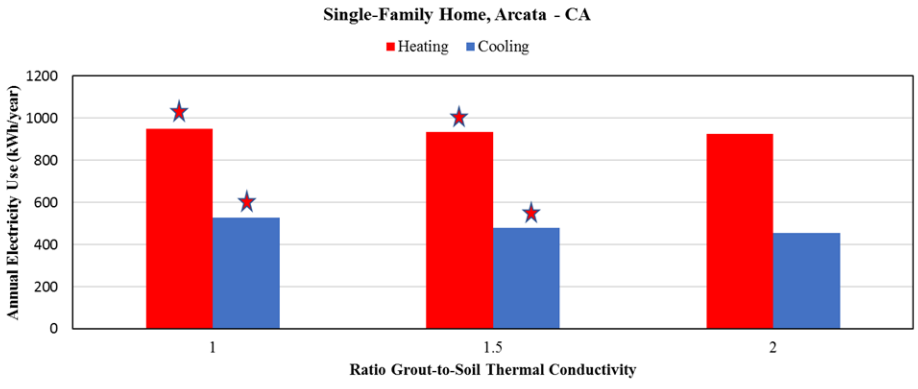

(**a**)

Figure 11. *Cont.*

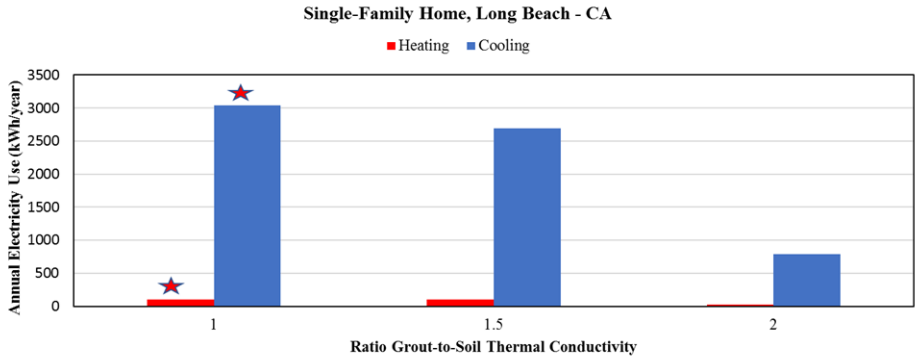

(**b**)

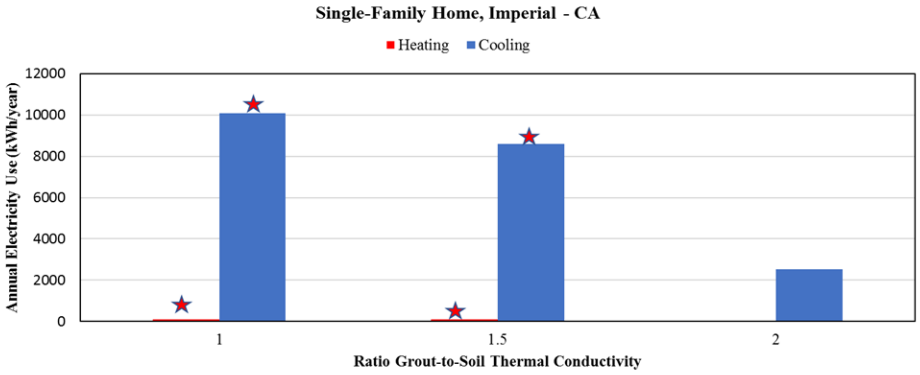

(**c**)

Figure 11. Impact of grout thermal conductivity on annual heating and cooling electricity end uses for 16 boreholes with 6.7 m (22 ft) depth when the prototypical house is located in (**a**) Arcata, (**b**) Long Beach, and (**c**) Imperial.

3.2.3. Effect of Borehole Depth

Two borehole depths are considered in this analysis to evaluate the performance of S-GSHP including 4.0 m (13 ft) and 6.7 m (22 ft). The results of the analysis are illustrated in Figure 12 showing the impact of the depth of 32 boreholes on the annual heating and cooling energy end uses for the prototypical house located in three CA locations. As expected, the deeper the boreholes, the more heat exchange capacity is available for the S-GSHP resulting in lower energy consumption especially for cooling as well as better operation temperature for the refrigerant. Specifically, increasing the borehole depth from 4 m (13 ft) to 6.7 m (22 ft) decreases annual cooling energy end use of the S-GHSP by 20% for Arcata, 27% for Long Beach, and 37% for Imperial. The heating energy use also decreases in all three locations but by merely 4% since the ground even at 4 m (13 ft) has a sufficient capacity to meet the house heating load.

Table 5 illustrates the performance of S-GSHP and deep GSHP systems when the house is in Long Beach. A set of combinations for both number and depth of boreholes is selected for this analysis to meet the heating and cooling thermal loads for the house. It is clear than only a limited number of deep boreholes for the conventional vertical GSHPs are needed to meet both the heating and cooling loads and perform similarly and even better than the shallow GSHPs with 32 boreholes and a depth of 6.7 m (22 ft). Specifically, a conventional GSHP with only 3 boreholes of 100 m depth consumes 3% less energy to heat and cool the house than the 32-borehole S-GSHP system.

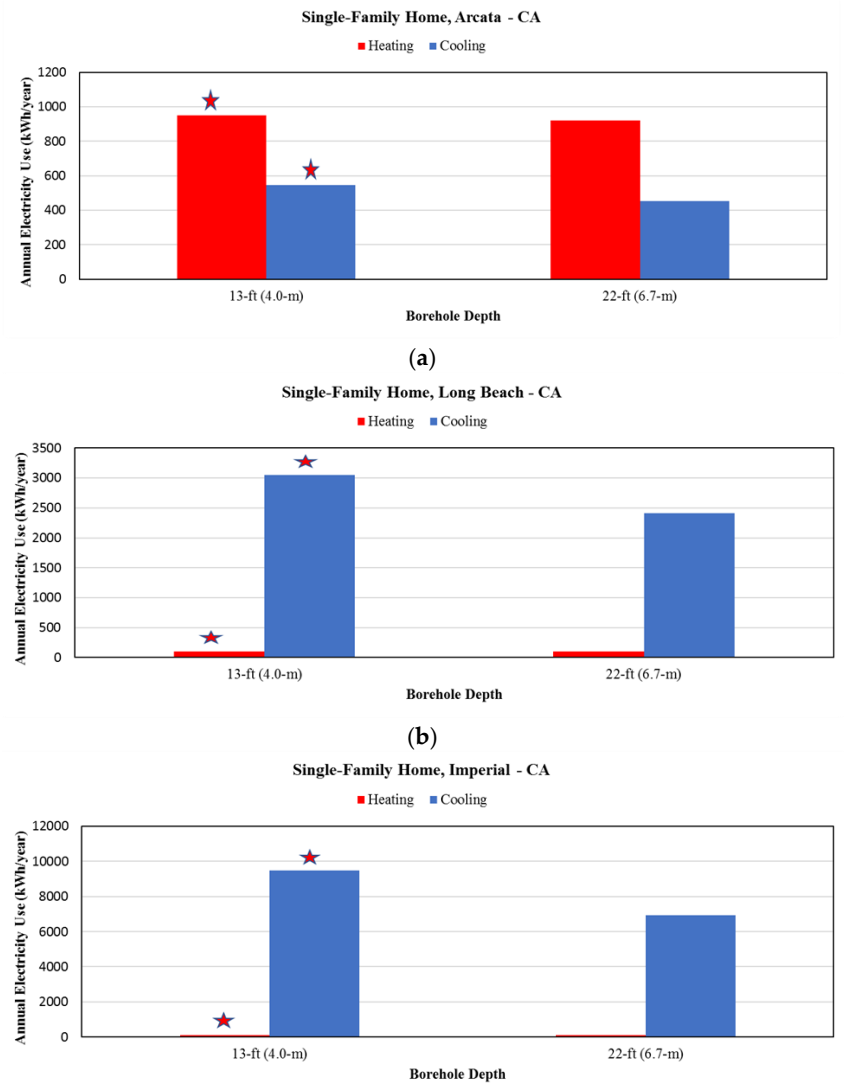

Figure 12. Impact of borehole depth on annual heating and cooling electricity end uses for 32 boreholes with 6.7 m (22 ft) depth when the prototypical house is located in (**a**) Arcata, (**b**) Long Beach, and (**c**) Imperial.

Table 5. Annual heating and cooling energy end uses for both deep and shallow GSHP systems when the house is located in Long Beach.

GSHP Type	Number of Boreholes/Depth	Annual Energy Use (kWh/Year)		Percent Difference Relative to 32/6.7 m S-GSHP Case (%)	
		Heating	Cooling	Heating	Cooling
Shallow	32/6.7 m	97.4	2420.6	0.0%	0.0%
	16/6.7 m	97.5	3054.2	0.1%	26.2%
	32/4.0 m	98.4	3051.2	1.1%	26.1%
Deep	2/75 m	93.5	3253.8	−4.0%	34.4%
	4/75 m	95.4	2429.8	−2.1%	0.4%
	2/100 m	95.4	2686.9	−2.0%	11.0%
	3/100 m	95.8	2345.4	−1.7%	−3.1%

4. Cost-Effectiveness Analysis

In this section, a cost-benefit analysis is conducted for S-GSHP configurations using two borehole depths. First, the installation costs for S-GSHP systems are estimated for two depths of the ground heat exchangers. Then, the energy savings associated with the deployment of S-GSHP instead of the baseline system HVAC are estimated. Finally, results of the life-cycle cost analysis are summarized to estimate the cost-effectiveness of the S-GSHP compared with baseline HVAC systems for all California climate zones.

4.1. Installation Costs of S-GSHP Systems

The installation costs of the S-GSHP systems are estimated based on reported data as detailed in Tables 6 and 7 respectively for 6.7 m (22 ft) S-GSHPs and 4.0 m (13 ft) configurations [54,55]. For these cost estimates, 4-ton capacity for the heat pumps is assumed in order to meet the heating and cooling loads for the prototypical single-family home considered in this study. Specifically, the cost of the heat pump is estimated to be USD 3000 [55] for all California locations.

Table 6. Total cost of S-GSHP systems using 6.7 m (22 ft) deep boreholes.

Cost Breakdown	Number of Boreholes				
	16	**24**	**32**	**40**	**48**
Heat pump equipment	3000	3000	3000	3000	3000
Borehole drilling	1056	1584	2112	2640	3168
Heat exchanger material	2800	4200	5600	7000	8400
Connections between heat pump and boreholes	230	346	461	576	691
Total installation cost	7086	9130	11,173	13,216	15,259
Federal tax credit (26%)	1842	2374	2905	3436	3967
Total cost (after tax credit)	5244	6756	8268	9780	11,292

Table 7. Total cost of S-GSHP systems using 4.0 m (13 ft) deep boreholes.

Cost Breakdown	Number of Boreholes				
	16	**24**	**32**	**40**	**48**
Heat pump equipment	3000	3000	3000	3000	3000
Borehole drilling	720	1080	1440	1800	2160
Heat exchanger material	2560	3840	5120	6400	7680
Connections between heat pump and boreholes	230	346	461	576	691
Total installation cost	6510	8266	10,021	11,776	13,531
Federal tax credit (26%)	1693	2149	2605	3062	3518
Total cost (after tax credit)	4818	6117	7415	8714	10,013

For the boreholes, the cost of drilling 6.7 m (22 ft) boreholes is estimated to be USD 66 per borehole while the cost for drilling 4.0 m (13 ft) boreholes is USD 45/borehole [54]. Moreover, the cost of the heat exchanger coils are determined to be USD 175/coil for the ground source heat-pump [54]. Thus, the total cost of the S-GSHP system depends on the number of ground heat exchanger loops required. Moreover, the cost of piping required to connect the various heat exchanger loops and heat pumps is estimated to be $USD 6.6/m (USD 2/ft). Moreover, the cost estimates for S-GSHPs consider the benefits associated with the geothermal systems using the federal tax credit of 26% of the total cost of the

equipment [56]. This tax credit reduces the overall installation costs as indicated in Table 6 for 6.7 m (2 ft) S-GSHPs and Table 7 for 4.0 m (13 ft) S-GSHPs.

4.2. Energy Savings Associated with S-GSHP Systems

To determine the cost-effectiveness of specifying S-GSHP systems to heat and cool residential buildings in California, the annual energy use reductions relative to the baseline HVAC systems (i.e., air-to-air heat pumps) are estimated for all California climate zones. These estimations are carried out using the simulation analysis results for both S-GSHP and baseline HVAC systems as discussed in Section 3. Several S-GSHP design configurations are considered in the analysis to account for the number and depth of boreholes. The results of the analysis are illustrated in Figure 13 showing the variation in S-GSHP energy savings relative to the baseline with the installation costs when the prototypical house is located in three California locations including (a) Arcata, (b) Imperial, and (c) Long Beach. The cost of the baseline HVAC system consisting of a 4-ton air source heat pump is estimated to be USD 4350 representing the average cost for an efficient heat pump [57]. As noted in Figure 13, all the S-GSHP configurations save annual HVAC energy consumption for homes located in Arcata. However, less than half of the S-GSHP configurations result in lower energy consumption relative to the baseline HVAC system for homes located in Imperial. For homes located in Long Beach, only one S-GSHP configuration consumes more energy than the baseline HVAC system.

4.3. Cost-Effectiveness of S-GSHP Systems

A life cycle cost analysis is performed to calculate the net present value (*NPV*) for installing S-GSHP instead of the baseline HVAC system for the prototypical house located in all 16 California climate zones. The NPV-based analysis can assess the cost-benefit of deploying the S-GSHP systems during their entire life cycle when compared with the performance of the baseline HVAC systems. The net present value (*NPV*) for S-GSHP with a varying number of boreholes is calculated for each location using Equation (9) [58]:

$$NPV = USPW \times \Delta EC - \Delta IC \tag{9}$$

where:

- ΔEC is the annual energy cost savings due to the deployment of S-GSHP instead of the baseline HVAC system. These savings are estimated based on annual energy consumption predicted by the simulation analysis as well as the residential electricity rates specific to the 16 California locations considered in this study [59].
- ΔIC is the incremental cost of installing S-GSHP instead of the baseline system (i.e., air source heat pump) as discussed in Section 4.1.
- *USPW* is the uniform series present worth factor expressed by Equation (10):

$$USPW = \frac{(1 - (1 + rd)^{-N}}{rd} \tag{10}$$

where N is the lifetime of the S-GSHP system, assumed to be 30 years in this analysis and r_d is the discount rate, set to be 5% for the study.

Table 8 summarizes the NPV results specific to 6.7 m (22 ft) S-GSHP design configurations for various borehole numbers. In particular, the results of Table 8 indicate that S-GSHPs are cost effective (i.e., NPV is positive) for locations where energy use savings can be achieved with a low number of boreholes compared with the baseline HVAC systems. S-GSHPs serving homes located in Mount Shasta are cost effective compared with the baseline HVAC systems regardless of the borehole number. Indeed, an annual energy cost saving of 20% is achieved by S-GSHP in this location, which compensates for the elevated installation costs even for large numbers of boreholes. However, these high installation costs affect the cost effectiveness of S-GSHPs for most California locations. Indeed, S-GSHP configurations with a borehole number exceeding 32 have negative NPV and thus are

not cost effective for all California locations except China Lake and Mount Shasta. For example, the deployment of S-GSHPs with 32 boreholes instead of the baseline HVAC systems for homes located in Long Beach results in 4% energy savings but requires a USD 8000 installation cost, which is almost double the cost of an air-source heat pump. The USD 4000 incremental costs of the S-GSHPs are too high to be recovered by the reduction in annual energy costs even during a 30-year period.

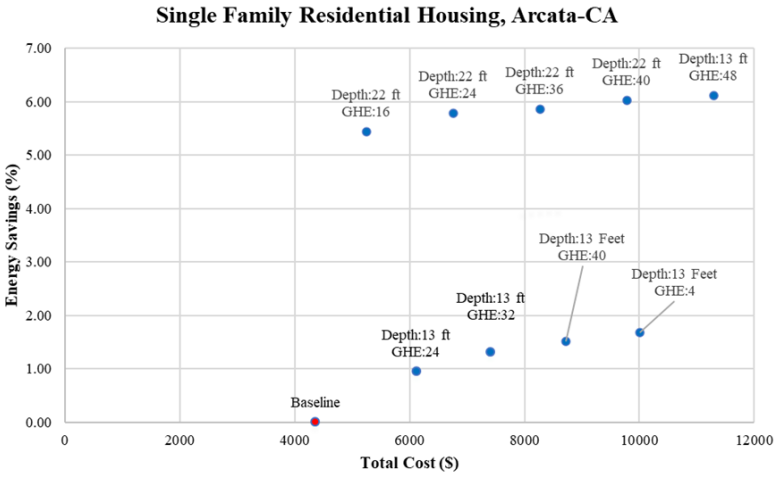

(**a**) Arcata.

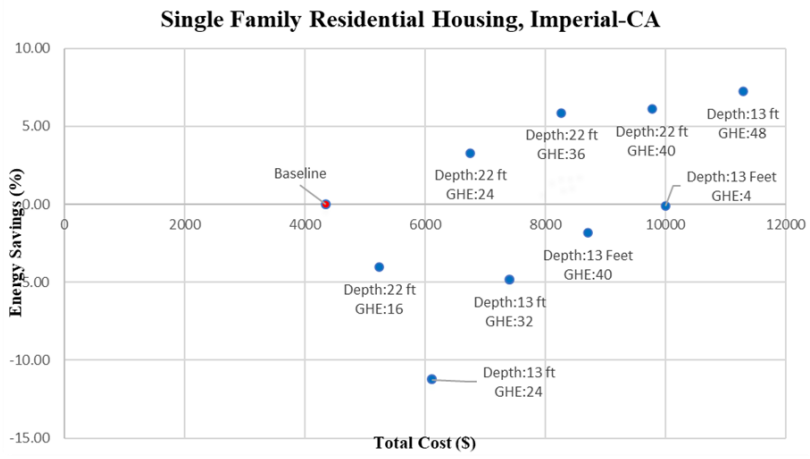

(**b**) Imperial

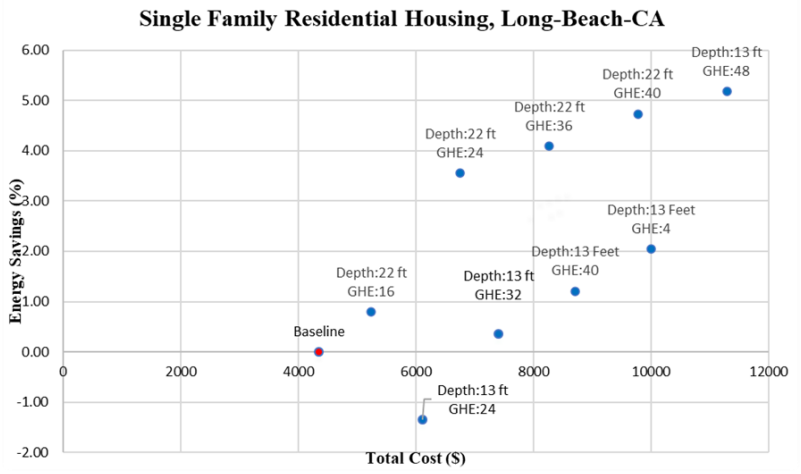

(**c**) Long-Beach

Figure 13. Energy savings vs. total cost for various configurations of S-GHSPs for three CA locations.

Table 8. NPV analysis results for S-GSHP systems with 6.7 m (22 ft) boreholes for 16 California locations.

Location	Electricity Rate (USD Cents/kWh)	Net Present Value of Savings (USD)				
		Number of Boreholes				
		16	**24**	**32**	**40**	**48**
Arcata	15.59	**1385**	−11	−1498	−2952	−4436
Burbank	14.81	−1459	−1493	−2518	−3693	−4885
China Lake	15.98	**461**	**2230**	**2079**	**1027**	−22
Fresno	15.59	−3189	−871	−1375	−2556	−3626
Fullerton	15.98	−1421	−1613	−2748	−3873	−5085
Imperial	16.35	−2432	−345	−464	−1420	−2233
Long Beach	15.98	−159	−685	−2004	−3287	−4636
March AFB	15.98	**94**	**159**	−780	−2000	−3176
Mount Shasta	13.1	**8791**	**8125**	**6938**	**5666**	**4346**
Oakland	15.59	**1189**	**26**	−1372	−2748	−4240
Red Bluff	15.59	**659**	**1472**	**945**	−249	−1370
Sacramento	12.39	**1768**	**1300**	**198**	−1140	−2422
San Diego	16.35	−468	−1312	−2568	−3867	−5155
San Jose	15.59	**830**	−170	−1532	−2873	−4262
Santa Maria	15.59	**1394**	**229**	−1135	−2498	−3909
Santa Rosa	15.59	**2071**	**1317**	**38**	−1278	−2606

Note: Bold values indicate positive NPV values.

On the other hand, S-GSHPs with 16 boreholes are cost-effective in most California locations except for climate zones of Burbank, Fresno, Fullerton, Imperial, Long-Beach, and San-Diego. For these locations, S-GSHPs do not achieve sufficient annual energy and cost savings to compensate for the installation costs. Using a similar cost-benefit analysis, the results indicate that S-GSHPs with a depth of 4.0 m (13 ft) are not cost-effective for all California locations except Mount Shasta due to the significantly lower annual energy savings compared with those achieved by the 6.7 m (22 ft) borehole systems as depicted in Figure 13.

5. Conclusions

In this paper, a systematic modeling approach for ground source heat pumps with shallow boreholes of less than 10 m is presented and is applied to assess their energy efficiency benefits to meet the heating and cooling needs of buildings. The modeling is based on the determination of G-functions estimated using a validated numerical model for shallow helical ground heat exchangers. These G-functions are then implemented in a whole-building simulation tool to determine the energy performance and cost benefits of shallow ground source heat pumps (S-GSHPs) to heat and cool buildings.

In this study, the flexibility of the modeling approach is applied to determine the optimal designs and cost effectiveness of S-GSHPs when deployed to residential buildings located in 16 California climate zones. The energy analysis includes the impacts of various design configurations for S-GSHPs depending on the depth and number of boreholes. Moreover, the cost benefit analysis assesses the economic feasibility of the S-GSHPs compared with the baseline heating and cooling systems consisting of air source heat pumps. The analysis results indicate that S-GSHPs can be economically competitive to air source heat pumps for selected California climate zones. Specifically, it is cost effective to use the S-GSHP in 10 out 16 California climate zones to provide heating and cooling for single family homes. In particular, S-GSHPs are better suited for climates where heating and cooling thermal loads are relatively balanced over the course of a year. In those climates, S-GSHPs can achieve energy savings when compared with air source heat-pumps, even with a limited number of ground heat exchangers as low as 16 boreholes. However, the

highest energy savings for S-GSHPs are achieved for locations with high heating demands (i.e., Arcata) while locations with dominant cooling needs (i.e., Oakland) exhibit lower energy reduction compared with the baseline HVAC systems.

Among all the 16 California locations considered in this study, the climate of Santa Rosa shows the maximum energy savings of 8.42% with a net present value (NPV) savings of USD 2000 when a S-GSHP with 6.7 m (22 ft) boreholes is used. While, the climate of Mount Shasta provides the highest NPV savings of USD 8000 for S-GSHP with 24 boreholes. Although the energy and cost savings are high for Mount Shasta, it should be noted that the land required to install 24 boreholes is significant. Hence, the feasibility of S-GSHPs depends not only on their cost-effectiveness compared with other HVAC systems but also on the availability of land for installing the needed boreholes. For heating- or cooling-dominated climates such as those of Burbank, Fresno, Fullerton, Imperial, and Red Bluff, energy savings can be achieved when the number of boreholes exceeds 16; however, due to the high installation costs, S-GSHPs are not economically feasible. Indeed, the energy cost savings for these locations are not sufficiently high to overcome the high S-GSHP installation costs even during a 30-year life cycle. Moreover, the analysis described in this report clearly indicates that S-GSHPs can be used as cost-effective alternatives to air-source heat pumps for 10 California climate zones especially when 16-borehole ground heat exchangers having a depth of 6.7 m (22 ft) are used. In addition, S-GSHPs allow for the electrification of homes as well as the reduction in carbon emissions when compared with other conventional heating and cooling systems.

Overall and more importantly, the study has demonstrated the flexibility of the modeling approach based on the G-function techniques and whole-building simulation tools to determine the annual energy performance and cost effectiveness of shallow helical ground heat exchangers to heat and cool buildings. While it is applied in this study for the specific case of homes in California, the presented modeling approach can be used for any building and location to assess the effectiveness of S-GSHPs as high-performance heating and cooling systems.

Author Contributions: Conceptualization, M.K. and J.H.; methodology, M.K.; software, A.S.; validation, A.S. and M.K.; formal analysis, M.K.; investigation, A.S.; resources, J.H.; data curation, A.S.; writing—original draft preparation, A.S.; writing—review and editing, M.K.; visualization, A.S.; supervision, M.K.; project administration, J.H.; funding acquisition, J.H. All authors have read and agreed to the published version of the manuscript.

Funding: This research was funded by University of California at Davis, WCEC, as a subcontract to grant EPC-15-019.

Acknowledgments: The authors acknowledge the technical support including evaluation of the G-function coefficients provided by A. Najib, V. Narayanan, and C. Harrington from UC Davis WCEC. This work has been partially supported by the California Energy Commission under a subcontract of grant CEC EPC-15-019.

Conflicts of Interest: The authors declare no conflict of interest. The funders had no role in the design of the study; in the collection, analyses, or interpretation of data; in the writing of the manuscript, or in the decision to publish the results.

Nomenclature

Acronyms

CA	California
COP	Coefficient of performance
CDD	Cooling degree days
CFD	Computational fluid dynamics
EER	Energy efficiency ratio
GSHP	Ground source heat pump
HDD	Heating degree days
HVAC	Heating ventilating and air conditioning

HVAC	Heating, ventilating, and air conditioning
S-GSHP	Shallow ground source heat pump
TAF	Thermo-active foundation
Symbols	
G_f	G function relating the fluid to the ground
G_b	G function relating borehole to the ground
He	Hessian function
N	Life cycle (years)
NPV	Net present value ($)
q_l	Thermal load (W)
$q_{l,j}$	Thermal load at time step j (W)
r	Radius of the cylindrical space variable (m)
r_d	Discount rate
$R_{e,b}$	Thermal resistance (°C/W)
t	Time (s)
T_f	Fluid temperature (°C)
T_g	Ground temperature (°C)
$USPW$	Uniform series present worth factor (years)
Greek Symbols	
Θ	Angle of the cylindrical space variable (rad)
ΔEC	Change in annual energy cost ($/year)
ΔIC	Change in implementation cost ($)
Δq_l	Change in heat transfer (W)
Δt	Time step (s)

References

1. Krarti, M. Ground-Coupled Heat Transfer. In *Advances in Solar Energy*; Goswami, D.Y., Ed.; ASES publication: Boulder, CO, USA, 1999; 90p.
2. Omer, A.M. Ground-source heat pumps systems and applications. *Renew. Sustain. Energy Rev.* **2008**, *12*, 344–371. [CrossRef]
3. EPA. *Renewable Heating and Cooling: Geothermal Heating and Cooling Technologies*; US Environmental Protection Agency: Washington, DC, USA, 2021. Available online: https://www.epa.gov/rhc/geothermal-heating-and-cooling-technologies (accessed on 30 March 2020).
4. Chauhan, A.; Kandlikar, S.G. Characterization of a dual taper thermosiphon loop for CPU cooling in data centers. *Appl. Therm. Eng.* **2019**, *146*, 450–458. [CrossRef]
5. Singh, R.M.; Sani, A.K.; Amis, T. *An Overview of Ground-Source Heat Pump Technology, Managing Global Warming*; Academic Press: Cambridge, MA, USA, 2018; pp. 455–485. [CrossRef]
6. Glassley, W.; Asquith, A.; Lance, T.; Brown, E. *Assessment of Califonia's Low Temperature Geothermal Resources: Evaluation of Geothermal Heat Pump System Use in California, Final Project Report by University of California at Davis for California Energy Commission*; Publication number: CEC-500-2014-060; California Energy Commission: Sacramento, CA, USA, 2012.
7. Rees, S.J. *Advances in Ground-Source Heat Pump Systems*; Woodhead Publishing: Cambridge, UK, 2016. [CrossRef]
8. Ma, Y.; Li, Y.Y.; Ma, Y.C.; Hu, X.F.; Hu, G.H. The Energy, Environmental and Economic Benefits Analysis of Ground-Source Heat Pump in Wuhan Region of Summer Condition. *Appl. Mech. Mater.* **2012**, *253-255*, 701–704. [CrossRef]
9. Michopoulos, A.; Voulgari, V.; Tsikaloudaki, A.; Zachariadis, T. Evaluation of ground source heat pump systems for residential buildings in warm Mediterranean regions: The example of Cyprus. *Energy Effic.* **2016**, *9*, 1421–1436. [CrossRef]
10. Bär, K.; Rühaak, W.; Welsch, B.; Schulte, D.; Homuth, S.; Sass, I. Seasonal High Temperature Heat Storage with Medium Deep Borehole Heat Exchangers. *Energy Procedia* **2015**, *76*, 351–360. [CrossRef]
11. Wang, Z.; Wang, F.; Liu, J.; Ma, Z.; Han, E.; Song, M. Field test and numerical investigation on the heat transfer characteristics and optimal design of the heat exchangers of a deep borehole ground source heat pump system. *Energy Convers. Manag.* **2017**, *153*, 603–615. [CrossRef]
12. Li, C.; Guan, Y.; Wang, X.; Zhou, C.; Xun, Y.; Gui, L. Experimental and numerical studies on heat transfer characteristics of vertical deep-buried U-bend pipe in intermittent heating mode. *Geothermics* **2019**, *79*, 14–25. [CrossRef]
13. Zhang, W.; Wang, J.; Zhang, F.; Lu, W.; Cui, P.; Guan, C.; Yu, M.; Fang, Z. Heat transfer analysis of U-type deep borehole heat exchangers of geothermal energy. *Energy Build.* **2021**, *237*, 110794. [CrossRef]
14. Liu, J.; Wang, F.; Gao, Y.; Zhang, Y.; Cai, W.; Wang, M.; Wang, Z. Influencing factors analysis and operation optimization for the long-term performance of medium-deep borehole heat exchanger coupled ground source heat pump system. *Energy Build.* **2020**, *226*, 110385. [CrossRef]
15. Esen, H.; Inalli, M.; Esen, M. Technoeconomic appraisal of a ground source heat pump system for a heating season in eastern Turkey. *Energy Convers. Manag.* **2006**, *47*, 1281–1297. [CrossRef]

16. Christodoulides, P.; Aresti, L.; Florides, G. Air-conditioning of a typical house in moderate climates with Ground Source Heat Pumps and cost comparison with Air Source Heat Pumps. *Appl. Therm. Eng.* **2019**, *158*, 113772. [CrossRef]
17. Wang, G.; Wang, W.; Luo, J.; Zhang, Y. Assessment of three types of shallow geothermal resources and ground-source heat-pump applications in provincial capitals in the Yangtze River Basin, China. *Renew. Sustain. Energy Rev.* **2019**, *111*, 392–421. [CrossRef]
18. Ooka, R.; Sekine, K.; Mutsumi, Y.; Yoshiro, S.; SuckHo, H. *Development of a Ground Source Heat Pump System with Ground Heat Exchanger Utilizing the Cast in Place Concrete Pile Foundations of a Building*; EcoStock 2007; The Richard Stockton College of New Jersey: Stockton, NJ, USA, 2007.
19. Lu, Q.; Narsilio, G.A.; Aditya, G.R.; Johnston, I.W. Economic analysis of vertical ground source heat pump systems in Melbourne. *Energy* **2017**, *125*, 107–117. [CrossRef]
20. Brandl, H. Energy foundations and other thermo-active ground structures. *Géotechnique* **2006**, *56*, 81–122. [CrossRef]
21. Sutman, M.; Speranza, G.; Ferrari, A.; Larrey-Lassalle, P.; Laloui, L. Long-term performance and life cycle assessment of energy piles in three different climatic conditions. *Renew. Energy* **2020**, *146*, 1177–1191. [CrossRef]
22. Jensen-Page, L.; Loveridge, F.; Narsilio, G.A. Thermal Response Testing of Large Diameter Energy Piles. *Energies* **2019**, *12*, 2700. [CrossRef]
23. Fadejev, J.; Simson, R.; Kurnitski, J.; Haghighat, F. A review on energy piles design, sizing and modelling. *Energy* **2017**, *122*, 390–407. [CrossRef]
24. Sani, A.K.; Singh, R.M.; Amis, T.; Cavarretta, I. A review on the performance of geothermal energy pile foundation, its design process and applications. *Renew. Sustain. Energy Rev.* **2019**, *106*, 54–78. [CrossRef]
25. Bourne-Webb, P.J.; Amatya, B.; Soga, K.; Amis, T.; Davidson, C.; Payne, P. Energy pile test at Lambeth College, London: Geotechnical and thermodynamic aspects of pile response to heat cycles. *Géotechnique* **2009**, *59*, 237–248. [CrossRef]
26. Knellwolf, C.; Peron, H.; Laloui, L. Geotechnical Analysis of Heat Exchanger Piles. *J. Geotech. Geoenvironmental Eng.* **2011**, *137*, 890–902. [CrossRef]
27. Wood, C.J.; Liu, H.; Riffat, S.B. An investigation of the heat pump performance and ground temperature of a piled foundation heat exchanger system for a residential building. *Energy* **2010**, *35*, 4932–4940. [CrossRef]
28. Cui, Y.; Zhu, J. Year-round performance assessment of a ground source heat pump with multiple energy piles. *Energy Build.* **2018**, *159*, 509–524. [CrossRef]
29. Alberdi-Pagola, M.; Poulsen, S.E.; Loveridge, F.; Madsen, S.; Jensen, R.L. Comparing heat flow models for interpretation of precast quadratic pile heat exchanger thermal response tests. *Energy* **2018**, *145*, 721–733. [CrossRef]
30. Krarti, M. *Thermo-Active Foundations for Sustainable Buildings, Monograph*; ASME Press: New York, NY, USA, 2015; 150p.
31. Zarrella, A.; Capozza, A.; De Carli, M. Performance analysis of short helical borehole heat exchangers via integrated modelling of a borefield and a heat pump: A case study. *Appl. Therm. Eng.* **2013**, *61*, 36–47. [CrossRef]
32. Dehghan, B.; Sisman, A.; Aydin, M. Parametric investigation of helical ground heat exchangers for heat pump applications. *Energy Build.* **2016**, *127*, 999–1007. [CrossRef]
33. Dehghan, B. Experimental and computational investigation of the spiral ground heat exchangers for ground source heat pump applications. *Appl. Therm. Eng.* **2017**, *121*, 908–921. [CrossRef]
34. Warner, J.; Liu, X.; Shi, L.; Qu, M.; Zhang, M. A novel shallow bore ground heat exchanger for ground source heat pump applications—Model development and validation. *Appl. Therm. Eng.* **2020**, *164*, 114460. [CrossRef]
35. Bertermann, D.; Klug, H.; Morper-Busch, L. A pan-European planning basis for estimating the very shallow geothermal energy potentials. *Renew. Energy* **2015**, *75*, 335–347. [CrossRef]
36. Bertermann, D.; Bernardi, A.; Pockelé, L.; Galgaro, A.; Cultrera, M.; de Carli, M.; Müller, J. European project "Cheap-GSHPs": Installation and monitoring of newly designed helicoidal ground source heat exchanger on the German test site. *Environ. Earth Sci.* **2018**, *77*, 180. [CrossRef]
37. Javadi, H.; Ajarostaghi, S.S.M.; Pourfallah, M.; Zaboli, M. Performance analysis of helical ground heat exchangers with different configurations. *Appl. Therm. Eng.* **2019**, *154*, 24–36. [CrossRef]
38. Rabin, Y.; Korin, E. Thermal analysis of a helical heat exchanger for ground thermal energy storage in arid zones. *Int. J. Heat Mass Transf.* **1996**, *39*, 1051–1065. [CrossRef]
39. Zarrella, A.; Emmi, G.; De Carli, M. Analysis of operating modes of a ground source heat pump with short helical heat exchangers. *Energy Convers. Manag.* **2015**, *97*, 351–361. [CrossRef]
40. Najib, A.; Zarrella, A.; Narayanan, V.; Grant, P.; Harrington, C. A revised capacitance resistance model for large diameter shallow bore ground heat exchanger. *Appl. Therm. Eng.* **2019**, *162*, 114305. [CrossRef]
41. Najib, A.; Zarrella, A.; Narayanan, V.; Bourne, R.; Harrington, C. Techno-economic parametric analysis of large diameter shallow ground heat exchanger in California climates. *Energy Build.* **2020**, *228*, 110444. [CrossRef]
42. Harrington, C.; Najib, A.; Narayanan, V.; Springer, D.; Slater, M.; Grant, P.; Liu, A.; Haile, J.; Krarti, M.; Huang, J. *Low Cost, Large Diameter Shallow Ground Loops for Ground-Coupled Heat Pumps*; Publication Number: CEC-500-2021-009; California Energy Commission: Sacramento, CA, USA, 2021.
43. DOE. *Residential Prototype Building Models, Build. Energy Codes Program*; US Department of Energy, 2020. Available online: https://www.energycodes.gov/\hskip1em\relaxdevelopment/residential/iecc_models (accessed on 25 November 2019).
44. Energyplus. EnergyPlusTM, Version 9.1.0, Documentation: Engineering Reference, US Department of Energy. 2019. Available online: https://energyplus.net/assets/nrel_custom/pdfs/pdfs_v9.1.0/EngineeringReference.pdf (accessed on 20 October 2019).

45. CEC. *Climate Zone Tool, Maps, and Information Supporting the California Energy Code*; California Energy Commission: Sacramento, CA, USA, 2021. Available online: https://www.energy.ca.gov/programs-and-topics/programs/building-energy-efficiency-standards/climate-zone-tool-maps-and (accessed on 20 November 2019).
46. Eskilson, P. Thermal Analysis of Heat Extraction Boreholes. Ph.D. Thesis, Department of Mathematical Physics, University of Lund, Lund, Sweden, 1987.
47. Yavuzturk, C.; Spitler, J.D. A short time step response factor model for vertical ground loop heat exchangers. *ASHRAE Trans.* **1999**, *105*, 465–474.
48. Yavuzturk, C.; Spitler, J.D.; Rees, S.J. A Transient Two-Dimensional Finite Volume Model for the Simulation of Vertical U-Tube Ground Heat Exchangers. *ASHRAE Trans.* **1999**, *105*, 475–485.
49. Kwag, B.C.; Krarti, M. Performance of Thermoactive Foundations for Commercial Buildings. *J. Sol. Energy Eng.* **2013**, *135*, 040907. [CrossRef]
50. Kwag, B.C.; Krarti, M. Evaluation of Thermo-Active Foundations for Heating and Cooling Residential Buildings. *J. Sol. Energy Eng.* **2016**, *138*, 061010. [CrossRef]
51. Kwag, B.C.; Krarti, M. Development of design guidelines for thermo-active foundations. *Indoor Built Environ.* **2018**, *27*, 805–817. [CrossRef]
52. Kwag, B.; Krarti, M. Evaluation of Interactions between Thermal Piles Integrated in Building Foundations. *J. Eng. Sustain. Build. Cities* **2020**, *1*, 031003. [CrossRef]
53. Li, M.; Lai, A.C. New temperature response functions (G functions) for pile and borehole ground heat exchangers based on composite-medium line-source theory. *Energy* **2012**, *38*, 255–263. [CrossRef]
54. Garcia, J.; Woolley, J.; Pistochini, T.; Baccei, B. *Performance Assessment of a Wide Diameter Shaloow Bore Ground Source Heat Exchanger*; Western Cooling Efficiency Center; University of California Davis; Sacramento Municipal Utility District: Sacramento, CA, USA, 2016. Available online: https://wcec.ucdavis.edu/wp-content/uploads/2016/06/SMUD-GSHE_Final-Report_2016.pdf (accessed on 10 April 2020).
55. PICKHVAC. Cooling and Heating Guide, Heat Pump Reviews and Prices. 2020. Available online: https://www.pickhvac.com/heat-pump/ (accessed on 10 April 2020).
56. Water-Furnace. Understanding the Federal Tax Incentives for Geothermal Heat Pumps. 2020. Available online: https://www.fiddelkehvac.com/Portals/0/products/brochures/HeatPump.pdf?ver=2020-01-23-140916-217 (accessed on 15 March 2020).
57. HomeAdvisor 2020. Heat Pump Prices of Installation and Replacement Costs. 2020. Available online: https://www.homeadvisor.com/cost/heating-and-cooling/install-a-heat-pump/ (accessed on 20 March 2020).
58. Krarti, M. *Energy Audit of Building Systems: An Engineering Approach*, 3rd ed.; CRC Press: Boca Raton, FL, USA, 2021.
59. Electricity Local California Electricity Rates. 2020. Available online: https://www.electricitylocal.com/states/california/ (accessed on 12 March 2020).